

## Optimisation of a dosing strategy for an HC-SCR diesel exhaust after-treatment system

Björn Westerberg<sup>a,b,\*</sup>, Christian Künkel<sup>c,d</sup>, C.U. Ingemar Odenbrand<sup>c</sup>

<sup>a</sup> Department of Chemical Reaction Engineering, Chalmers University of Technology, SE-412 96 Göteborg, Sweden

<sup>b</sup> Department of Engineering, Physics and Mathematics, Mid Sweden University, SE-891 18 Örnköldsvik, Sweden

<sup>c</sup> Department of Chemical Engineering II, Lund University, P.O. Box 124, SE-221 00 Lund, Sweden

<sup>d</sup> Scania CV AB, SE-151 87 Södertälje, Sweden

Received 24 March 2001; accepted 27 August 2001

### Abstract

Several principal aspects and components of an advanced catalytic exhaust after-treatment system for NO<sub>x</sub> reduction on a heavy-duty diesel truck engine have been systematically examined and evaluated. The after-treatment system consists of de-NO<sub>x</sub> catalysts, injection of a reducing agent (diesel fuel), and computer programs to model the engine and catalysts in real time. These models are combined with a third program, a strategy, to control the injection of reducing agent during transient operation. Evaluation of the system was performed using the standard European transient cycle (ETC). The benefits and disadvantages of an oxidation catalyst upstream the reductant injection are clarified. Whereas an increased NO<sub>2</sub>/NO ratio is beneficial at larger reductant dosages, the effects of temperature levelling and delay are detrimental for system performance. The dynamic effect of introducing a strategy for distributing the reducing agent in time is elucidated. The strategy itself is presented and the process of its systematic optimisation is closely followed. Implications of the optimisation are that catalyst temperature is the most important variable in the strategy. Also, a considerable part of the reducing agent should be distributed at low and intermediate temperatures, for utilising an increased NO<sub>2</sub>/NO ratio. Furthermore, results suggest that a smooth, rather than instantaneous, adjustment of reductant dosage to driving conditions is necessary. Finally, a set-up with two injectors is examined for its potential in the application. It is shown to be of disadvantage for the ETC as a whole, but may not be so at lower exhaust gas flows. © 2002 Published by Elsevier Science B.V.

**Keywords:** After-treatment system; NO<sub>x</sub> reduction; European transient cycle

### 1. Introduction

The demand for catalytic NO<sub>x</sub> after-treatment for diesel vehicles is commonly recognised. Due to the engine construction, NO<sub>x</sub> is the only major diesel exhaust gas pollutant, the removal of which cannot proceed efficiently with a passive after-treatment system. The diesel engine is, however, one of the most efficient energy converters of today, with up to 50% of the chemically bound fuel energy transformed into kinetic energy. The incentive to continue using the engine is thus large, despite its emission characteristics.

Primary measures against NO<sub>x</sub> emissions, i.e., modifications of engine construction such as exhaust gas recirculation (EGR) or retarded injection timing, tend to affect the engine efficiency and/or life span negatively. These measures also

most likely fail to fulfil the legislative demands in Europe of 2.0 g NO<sub>x</sub>/kW h for heavy-duty diesel emissions by 2008.

HC-SCR (HydroCarbon-SCR), the use of a hydrocarbon-based reducing agent (especially the fuel already onboard) for NO<sub>x</sub> reduction in oxygen excess, has attracted much interest during the last few years. The fact relies partly on the wish of avoiding the problem of infrastructure needs related with other types of SCR (i.e. ammonia or urea SCR). A vast number of investigations of HC-SCR have been carried out, most of which using synthetic exhaust gases in laboratory scale, e.g. [1,2]. Experimental work with real exhaust gas under steady-state conditions have been published to a much more limited extent [3–6]. Both of these types of tests may be very helpful in screening of catalysts and examination of mechanisms. They do, however, fail to predict performance under realistic conditions for the application the catalysts are meant for, and give little information on how to use the catalysts' specific performance under different circumstances. In transient use, driving conditions vary unpredictably, causing temperatures, mass flow and NO<sub>x</sub>

\* Corresponding author. Present address: Department of Chemical Reaction Engineering, Chalmers University of Technology, SE-412 96 Göteborg, Sweden.

E-mail address: bjorn@cre.chalmers.se (B. Westerberg).

concentrations to fluctuate widely. In turn, any active emission control system must have the ability to predict conditions in the exhaust gas and in the catalysts. Moreover, these predictions need interpretation to yield, at any given moment, an optimal reductant dosage upstream the catalysts. The optimal dosage should be calculated according to a strategy adapted to engine characteristics, catalyst characteristics, and emission demands to achieve a limited use of reductant, i.e., diesel fuel. Some publications report control of transient systems, however, mainly limited to pre-defined cycles [7–9], using a time-controlled, constant or semi-constant dosage of reductant. Semi-constant dosage may, e.g., be proportional to engine load or fuel consumption. Such systems are unlikely to reach the performance called for by legislation and consumer society. Very few authors have previously reported on integrated systems based on elaborate kinetics and dosing strategies [10,11].

This paper presents an investigation of a complete system for  $\text{NO}_x$  control, capable of realistic use as represented by the standard European transient cycle (ETC). The system consists of high temperature (HT) catalysts, where the main part of the  $\text{NO}_x$  reduction occurs, and low temperature (LT) catalysts, where CO and HC are oxidised to  $\text{CO}_2$ . The effects of important parameters for such a system, in both hardware and software, are elucidated. These parameters are:

1. The benefits of an increased  $\text{NO}_2/\text{NO}$  ratio. These have previously been investigated in laboratory scale by a number of authors, e.g. [12–14]. Its application and implied effects in realistic conditions have, however, not previously been examined.
2. The effect of temperature levelling and delay in the system. The reason for this examination is that an increased  $\text{NO}_2/\text{NO}$  ratio is normally achieved by the introduction of an extra catalyst with oxidative properties. Furthermore, the effect is also of importance for applications with multiple reductant injectors.
3. The dosing strategy and its components. These factors determine the cost efficiency of an active  $\text{NO}_x$  after-treatment system. An optimisation of the dosing strategy regarding  $\text{NO}_x$  reduction relative to the reductant consumption is performed and its implications are interpreted.
4. The effect of multiple injectors. Earlier findings [15] suggest that a multiple injection of reductant along the catalyst system may be of advantage in some situations. The advantage over a single injector set-up may partly lie in the improved distribution of reducing agent along the system axis, and partly in the possibility of dosing reducing agent at catalyst sections with preferred temperatures.

System dynamics is accounted for by the system and its optimisation is based on earlier work [10,15–17]. In this investigation only  $\text{NO}_x$  reduction is considered. The topic of HC, CO and  $\text{N}_2\text{O}$  emissions is addressed in a previous publication [15].

## 2. Experimental methods

### 2.1. Engine, fuel, catalysts and reductant injection

All experiments were performed on a 6.71 Volvo TD73 EA heavy-duty diesel engine placed in a rig capable of performing transient cycles. Swedish MK1, a commercial low-sulphur fuel (approx. sulphur content: 5–10 ppm), was used both as engine fuel and reducing agent. Monolithic catalytic converters supplied by Johnson Matthey were connected to the exhaust pipe for the simultaneous removal of  $\text{NO}_x$ , CO and HC. Most of the catalyst volume consisted of a high temperature active (HT) catalyst providing the major conversion of  $\text{NO}_x$ . A smaller portion of the catalyst volume consisted of a low temperature active (LT) catalyst, which was also used for removing residual HC and CO. The injectors consisted of air-assisted spray nozzles. Further information on injectors and their performance in this application can be found elsewhere [15].

### 2.2. Test procedures

The exhaust gas system with its three different catalyst set-ups was according to Fig. 1. Fifteen litres of the catalyst volume consisted of HT monoliths. 2.5 l of the catalyst volume consisted of an LT monolith. In designated tests one extra monolith (5 l HT or LT) was placed upstream the remainder of the whole system, including HC injection. The location of the catalysts and the injection of diesel fuel into the exhaust gas stream were as shown in Fig. 1.

All experiments were performed as standard ETCs. Cycles were performed with intervening gaps of approx. 7 min. In order to facilitate the following interpretation of results, engine characteristics during the ETC, such as speed, torque, mass flows and temperature, can be found in Fig. 2.

The ETC is an adequate and widely used means for comparison of engine and after-treatment performance. However, it is essential to be aware of limitations of interpretation introduced with the test method. Firstly, all modes in the test cycle depend on each other since the test cycle lasts only 30 min, and the subcycles of urban, extraurban and motorway traffic are limited to 10 min each. Secondly, the ETC does not reflect the actual use of any single vehicle, which varies enormously depending on the application of the vehicle is intended for. Given the dynamics of the examined and similar systems it is of importance not to draw too far-reaching conclusions from the limited model of reality a test cycle such as the ETC provides.

### 2.3. Exhaust gas analysis

Sampling of the exhaust gas was carried out according to Fig. 1. The sampled gas was conducted through heated ( $190^\circ\text{C}$ ) PTFE pipes to a J.U.M. Engineering model 222 heated gas pre-filter. The HC content was determined using

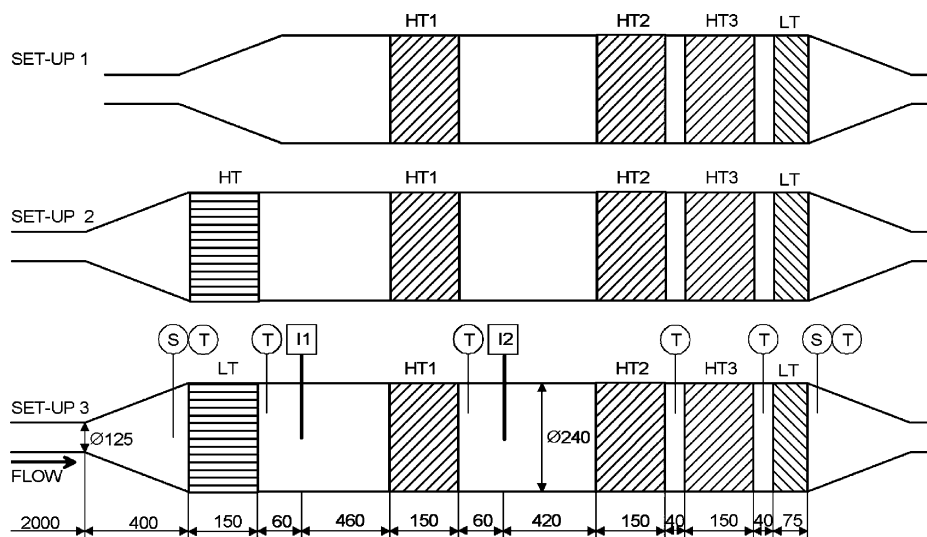


Fig. 1. Catalyst configurations. Measures and auxiliary equipment indicated on set-up 3. I: injector, S: sampling point, T: thermocouple. All measures in mm.

a J.U.M. Engineering model VE5 FID instrument. An Eco-Physics CLD 700 RE ht chemiluminescence instrument was used for  $\text{NO}_x$  analysis, and a Siemens Ultramat 22P for CO analysis.  $\text{N}_2\text{O}$  was analysed with a Siemens Ultramat 5E. Water in the gas for CO and  $\text{N}_2\text{O}$  analysis was condensed using a Siemens 7 MB gas cooler.

#### 2.4. Dosing strategy

The dosing strategy determines the amount of diesel to be injected into the exhaust gas stream. The dosing strategy takes into account the catalyst temperature and the  $\text{NO}_x$  flow, where calculation of the amount of injected hydrocarbons,  $F_{\text{inj}}$ , through a momentary fuel penalty,  $P_F$ , forms the core of the strategy.

$$F_{\text{inj}} = P_F F_B \quad (1)$$

$F_B$  is the fuel flow. The term “momentary fuel penalty” should be understood as a reductant dose equivalent to a certain fraction of the engine fuel consumption at any given point of time. The momentary fuel penalty has a physical meaning in that the  $\text{NO}_x$  flow is almost proportional to the engine fuel flow. The reason for using a momentary fuel penalty is to have a strategy, i.e., generally applicable and valid not only for a certain test cycle. A cumulative fuel penalty of comparable size could thus be obtained independent of test cycle type. The momentary fuel penalty is determined from the following function:

$$P_F = P_0 + B(T)\{k_0 + k_1 F_{\text{NO}_x} + k_2 F_{\text{NO}_x}^2\} \quad (2)$$

$P_0$  is a base level fuel penalty and  $B(T)$  is a barrier function that takes into account the temperature characteristics of the catalyst.  $k_0$ ,  $k_1$  and  $k_2$  all determine the level of the temperature-dependent part of the momentary fuel penalty, which thus may have zero, linear or quadratic dependence of the  $\text{NO}_x$  flow,  $F_{\text{NO}_x}$ , which may also be viewed as a  $\text{NO}_x$  reduction potential. The barrier function is defined by the actual catalyst temperature,  $T$ , a barrier temperature,  $T_B$ , and a steepness parameter,  $n_S$ :

$$B(T) = 1 - e^{-[T/T_B]^{n_S}} \quad (3)$$

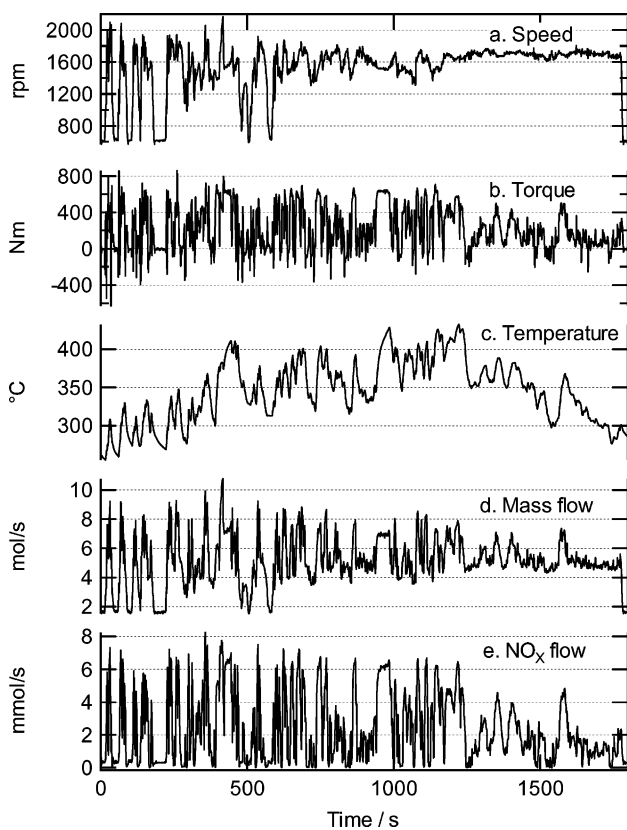


Fig. 2. (a) Speed, (b) torque, (c) engine out temperature, (d) mass flow and (e)  $\text{NO}_x$  flow during an ETC.

The dosing strategy has a similar appearance as in an earlier work [15]. The difference consists of two new terms; the quadratic dependence of the  $\text{NO}_x$  flow,  $k_2$ , and the base level fuel penalty,  $P_0$ . In the earlier work, the linear dependence of  $\text{NO}_x$  flow proved beneficial. The quadratic dependence of the  $\text{NO}_x$  flow was added in order to investigate whether a higher order dependence of the  $\text{NO}_x$  flow was beneficial or not. The reason for adding a base level fuel penalty was to utilise the increased  $\text{NO}_x$  conversion obtained at lower temperatures when using an oxidation catalyst to increase the  $\text{NO}_2$  content upstream the injection of reductant.

When two injectors were used, two momentary fuel penalties,  $P_{F1}$  and  $P_{F2}$ , were calculated. For  $P_{F1}$ ,  $T$  in Eq. (3) was the temperature in the catalyst downstream the first injector, for  $P_{F2}$  the temperature in the catalyst downstream the second injector was used. A distribution factor,  $f_D$ , determined the actual amounts of injected hydrocarbons,  $F_{inj1}$  and  $F_{inj2}$ , from injectors 1 and 2 according to

$$F_{inj1} = \{P_{F1} + (1 - f_D)P_{F2}\}F_B \quad (4)$$

$$F_{inj2} = f_D P_{F2} F_B \quad (5)$$

### 2.5. Engine and catalyst models

The engine model consists of a map from which all raw emissions and flows are interpolated linearly [15]. As input to the catalyst model, the temperature upstream for all monoliths was used during evaluation of different catalyst configurations. The reason was to avoid influence on the dosage from temperature levelling and delaying effects when comparing different catalyst configurations. In all other tests, the temperature at the first injector was used. The catalyst model is used for determining the monolith temperature, which, in turn, is used by the dosing strategy to determine the amount of hydrocarbon to inject. The monolithic catalyst is modelled with mass and heat balances as a series of 10 continuously stirred tanks. The fundamentals of the catalyst model, including a validation of the thermal part, are given in other publications [16,17]. The standard deviation for the temperature residual during a ETC was determined to  $3.9^\circ\text{C}$  [17].

### 2.6. Evaluation of catalyst configurations

Two kinds of experiments were performed for evaluating the performance of different catalyst configurations. Firstly, experiments with a constant momentary fuel penalty of 0, 1, 3 and 5%. Secondly, one experiment with a reference dosing strategy. In the reference dosing strategy, the parameter values were:  $P_0 = 0$ ,  $T_B = 360^\circ\text{C}$ ,  $n_S = 5$ ,  $k_1 = 4$ ,  $k_2 = 0$ . This set of parameter values made the dosing strategy equal to the strategy that showed best performance in an earlier work [15] where no oxidation catalyst upstream the injector was used.

### 2.7. Evaluation of dosing strategy

A coarse optimisation of the dosing strategy was performed. The purpose of the optimisation was not only to improve the dosing strategy but also to gain a better understanding of which properties of the dosing strategy are important. The starting point for the optimisation was the parameter values used in the reference dosing strategy (defined above). In order to reduce the number of experiments reduced factorial designs were used. In each experimental design three of the parameters were studied. One experiment was performed in the centre point. This resulted in five experiments for each experimental design. For each experiment the parameter  $k_0$  was set in order to yield a predicted cumulated fuel penalty of 5%. The response was the cumulated  $\text{NO}_x$  conversion adjusted to 5% cumulated fuel penalty. After each experimental design, the influence of each studied parameter was determined by fitting a linear model. Experiments were then performed in the direction of the steepest ascent. From these experiments a better set of parameters was obtained, around which a new experimental design then was centred.

## 3. Results and discussion

Performing and interpreting experiments with increased  $\text{NO}_2/\text{NO}$  ratio is relatively easy in laboratory scale. In real systems, however, an increased  $\text{NO}_2/\text{NO}$  ratio is normally obtained by introducing an oxidation catalyst upstream the remainder of the system. As side effects at least two phenomena occur: unburned HC and CO from the engine combustion process are oxidised to  $\text{CO}_2$  in the catalyst, and transient temperature variations are levelled and delayed. In order to distinguish the first effect from the second, three sets of experimental set-ups were used, see Fig. 1. Set-up 1 contained no extra catalyst, set-up 2 contained an HT catalyst upstream all other catalysts, whereas set-up 3 contained an LT catalyst replacing the HT catalyst of set-up 2. The comparison of set-ups 1 and 2 allowed the study of temperature effects alone, since the HT catalyst in the absence of large amounts of HC has a negligible effect on exhaust gas composition. The examination of these two factors is accounted for under the headings “effects of temperature levelling and delay” and “effect of an oxidation catalyst”.

The application of a  $\text{NO}_x$  reduction system in a transient environment introduces the problem of distributing the reductant for optimal performance, in this case  $\text{NO}_x$  reduction during an ETC. This topic is elucidated in the sections “dynamic effect of the dosing strategy” and “optimisation of the dosing strategy”. Previous work [15] indicated the benefit of injecting reductant at multiple points in the exhaust system. Therefore, the dosing strategy allows for dual injectors, and this feature is examined in the section “introduction of multiple injectors”.

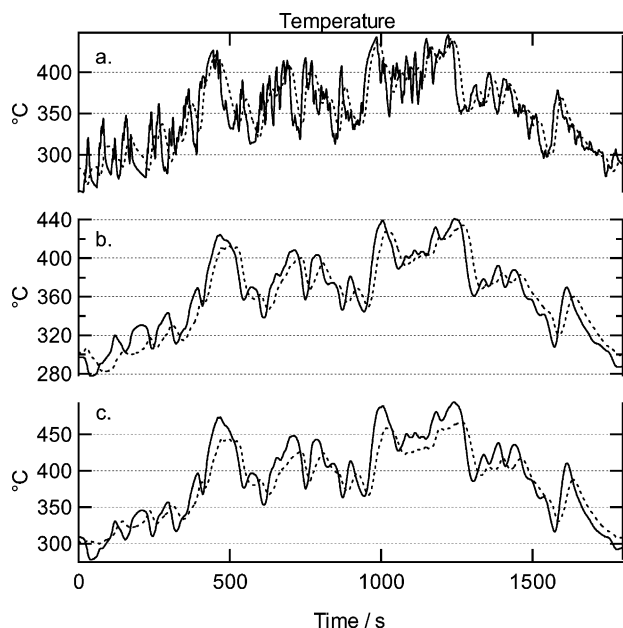


Fig. 3. Temperature with set-up 1 (solid) and 2 (dotted): (a) at injector and downstream HT1, (b) with no dosage and (c) with 5% momentary fuel penalty.

### 3.1. Effects of temperature levelling and delay

The exhaust gas temperature at the injector is, as seen in Fig. 3a, slightly levelled and delayed for set-up 2 compared to set-up 1, as can be expected. Temperatures are, however, essentially the same. The same trends are obvious in Fig. 3b regarding temperature downstream HT1 with no reductant dosage. Introduction of a 5% momentary fuel penalty does, however, lead to rather dramatic changes in the temperature profiles downstream HT1 (Fig. 3c). In set-up 1, temperatures rise sharply to a level of intermittently more than 30 °C higher than in set-up 2. This is especially valid between 420–500 and 950–1250 s, two periods where NO<sub>x</sub> emissions are relatively large due to high engine load.

The effect of a strategy upon introduction of an extra monolith is shown in Fig. 4. Accumulated NO<sub>x</sub> conversion for momentary fuel penalties in set-ups 1 and 2 (Fig. 4a) show a good correlation with the occurrence of relatively high NO<sub>x</sub> flow and high temperature situations (e.g., 420–500 and 950–1250 s). For the set-ups with 0 and 1% momentary fuel penalty, the difference in NO<sub>x</sub> conversion is very small. Set-up 1 is, however, superior to set-up 2 with respect to NO<sub>x</sub> emissions during the experiments with 3 and 5% momentary fuel penalty. Compared with a 5% momentary fuel penalty, the strategy yields a larger dosage during 400–500 and 950–1250 s (Fig. 4b), and less at other times.

High load and moderate speeds often occur simultaneously, for example at accelerations, thus causing relatively high mass flows, high temperatures and large NO<sub>x</sub> emissions. In other words, the potential to reduce NO<sub>x</sub> emissions lie in utilising the high temperatures for catalytic reduction

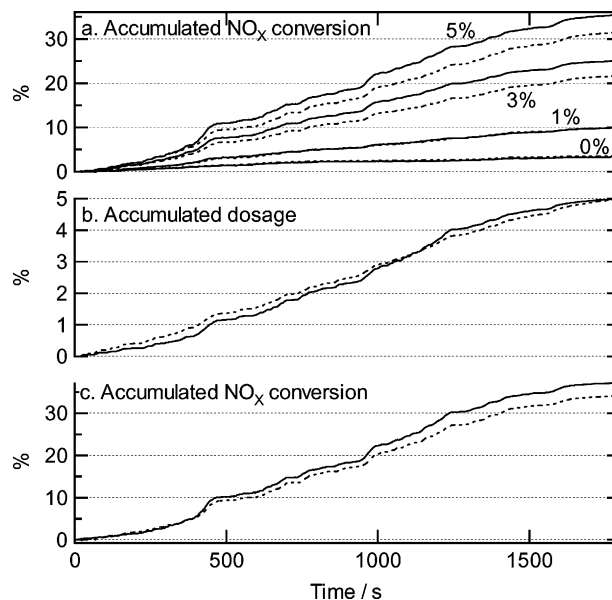


Fig. 4. (a) Accumulated NO<sub>x</sub> conversion with 0, 1, 3 and 5% momentary fuel penalty for set-up 1 (solid) and 2 (dotted), (b) accumulated dosage with 5% momentary fuel penalty (dotted) and with reference dosing strategy (solid) and (c) accumulated NO<sub>x</sub> conversion with the reference dosing strategy for set-up 1 (solid) and 2 (dotted).

when the NO<sub>x</sub> flow is large. In a configuration such as set-up 2 the task is more demanding than with set-up 1, since, due to the temperature delay, NO<sub>x</sub> flow and high temperature are no longer necessarily accompanied. For the set-ups with 0 and 1% momentary fuel penalty, the difference in dose pattern with and without strategy is too small to significantly influence NO<sub>x</sub> conversion.

The effect of a temperature levelling catalyst brick on NO<sub>x</sub> conversion is also clearly visible in Fig. 4c, where, congruent with the above reasoning, performance is better for set-up 1 than for set-up 2. The differences are more expressed at times of high load engine operation (400–500 and 950–1250 s). It must, however, be noted that the strategy is exactly the same for the two cases, and thus neither set-up is optimised.

### 3.2. Effect of an oxidation catalyst

A very interesting feature of the comparison of set-ups 2 and 3 in Fig. 5a is that whereas set-up 2 is favourable at lower dosages (1% momentary fuel penalty), set-up 3 shows advantage at larger dosages (5% momentary fuel penalty).

The cause is found in the removal of HC and CO from the exhaust gas upstream reductant injection together with the elevated NO<sub>2</sub>/NO ratio. The phenomena render the HT catalysts more thoroughly oxidised through the lowering of HC concentration and the oxidation of HC species by NO<sub>2</sub>. The oxidised surface of the HT catalyst causes a small unselective combustion of HC, and only doses exceeding this HC consumption result in NO<sub>x</sub> conversion. There is thus

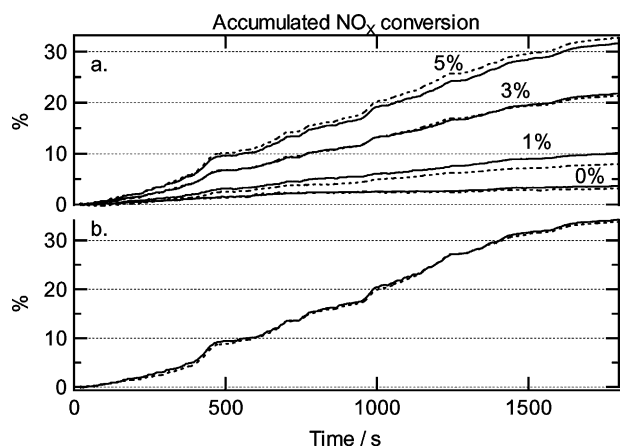


Fig. 5. (a) Accumulated NO<sub>x</sub> conversion with 0, 1, 3 and 5% momentary fuel penalty for set-up 2 (solid) and 3 (dotted), (b) accumulated NO<sub>x</sub> conversion with reference dosing strategy for set-up 2 (solid) and 3 (dotted).

a threshold value for the dose above which NO<sub>x</sub> reduction benefits from NO pre-oxidation. One can also note [17] that a significant phenomenon of NO<sub>x</sub> desorption without subsequent reduction exists, a desorption resulting from small HC doses at elevated NO<sub>2</sub>/NO ratios.

Differences in reference strategy dosage between set-ups 2 and 3 are very small since temperature differences between the two set-ups are negligible. Accumulated NO<sub>x</sub> conversion using the reference strategy (as shown in Fig. 5b) shows small differences in set-up 2 compared to set-up 3. No larger differences are expected, since the strategy is not adapted to the conditions supplied by set-up 3.

An observation well worth making is that set-up 3 in all cases implies a two-step reduction, whereas 1 and 2 do not. The NO<sub>x</sub> reduction occurring with unburned engine HC emissions alone will in set-up 3 take place in the extra LT monolith, situated upstream all injectors. In 1 and 2, this reduction will take place in the downstream HT and LT monoliths.

### 3.3. Dynamic effect of the dosing strategy

When using a dosing strategy, the injection of hydrocarbons/reductant varies continuously during the test cycle. Due to the accumulation of reactants on the catalyst, the response from a change in injection cannot be expected to be immediate. A certain time is needed before the whole catalyst monolith has adjusted to a new injection level. In order to determine which influence this dynamic effect has on the NO<sub>x</sub> conversion, a comparison was made between the actual NO<sub>x</sub> conversion obtained with dosing strategy and the NO<sub>x</sub> conversion obtained when interpolating between experiments performed with different constant momentary fuel penalties. In Fig. 6, the actual and the interpolated cumulated NO<sub>x</sub> conversions during a test cycle are shown. The total actual NO<sub>x</sub> conversion is 33.9% and the total

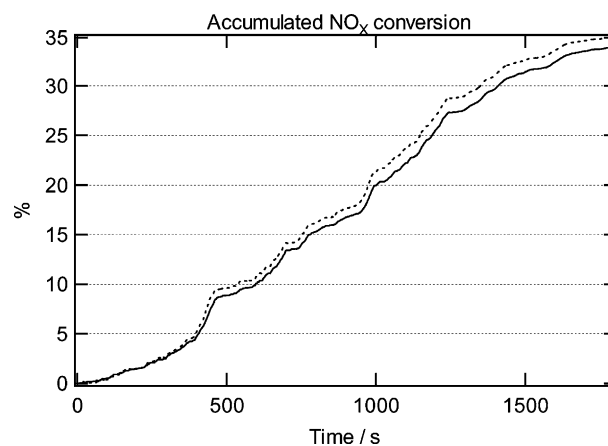


Fig. 6. Accumulated NO<sub>x</sub> conversion for the reference dosing strategy with set-up 3 (solid). Accumulated NO<sub>x</sub> conversion obtained by interpolation between tests run with constant momentary fuel penalty (dotted).

interpolated NO<sub>x</sub> conversion is 34.9%. The gap between actual cumulated NO<sub>x</sub> conversion and interpolated cumulated NO<sub>x</sub> conversion is increasing during most of the cycle and especially around 420 and 960s. At these instances, the engine is running at a high load and the dosing strategy gives a large injection. The time needed for the catalyst monolith to adjust to a new injection level is thus significantly longer than 1s, the length of each step in the ETC test. This indicates that an efficient dosing strategy should yield a smooth dosage rather than change the dose instantly with the driving conditions.

### 3.4. Optimisation of the dosing strategy

The objective function subject to optimisation was cumulated NO<sub>x</sub> conversion over an ETC. In the first experimental design, the influences of  $k_1$ ,  $n_S$  and  $T_B$  were studied. In Table 1, the values of the studied parameters and the obtained responses are listed.

The influence of each parameter was determined by least squares fitting of a linear model:

$$\hat{y}_1 = 33.86 - 0.0650x_{11} - 0.2575x_{12} + 0.0275x_{13} \quad (6)$$

The first model (Eq. (6)) indicated that  $k_1$  had a weak negative influence, that  $n_S$  had a strong negative influence, and that  $T_B$  had a weak negative influence on NO<sub>x</sub> conversion. By changing the parameters in the direction of the steepest ascent a more optimal set of parameter values should be obtained. In this case it should have meant mainly a decrease of  $n_S$ , resulting in a more even distribution of the reducing agent during the cycle. However, this could also be obtained by using a non-zero value of  $P_0$ . The latter action was preferred because a decrease in  $n_S$  would have lessened the significance of  $T_B$ , restricting further optimisation of this parameter. Thus, instead of changing the parameters in the direction of the steepest ascent, where  $n_S$  and  $T_B$  kept unchanged,  $k_1$  was decreased and  $P_0$  set to 0.0025. A new

Table 1  
Variables and responses for the first experimental design<sup>a</sup>

Variables			Normalised and centred variables			NO <sub>x</sub> conversion, y <sub>1</sub>
<i>k</i> <sub>1</sub>	<i>n</i> <sub>S</sub>	<i>T</i> <sub>B</sub> (°C)	<i>x</i> <sub>11</sub>	<i>x</i> <sub>12</sub>	<i>x</i> <sub>13</sub> = <i>x</i> <sub>11</sub> <i>x</i> <sub>12</sub>	
4	5	360	0	0	0	33.72
3	2	375	−1	−1	1	34.24
3	8	345	−1	1	−1	33.68
5	2	345	1	−1	−1	34.06
5	8	375	1	1	1	33.60

<sup>a</sup> Fixed parameters were  $P_0 = 0$  and  $k_2 = 0$ .  $x_{11}$ ,  $x_{12}$  and  $x_{13}$  represents the normalised and centred variables  $k_1$ ,  $n_S$  and  $T_B$ , respectively.

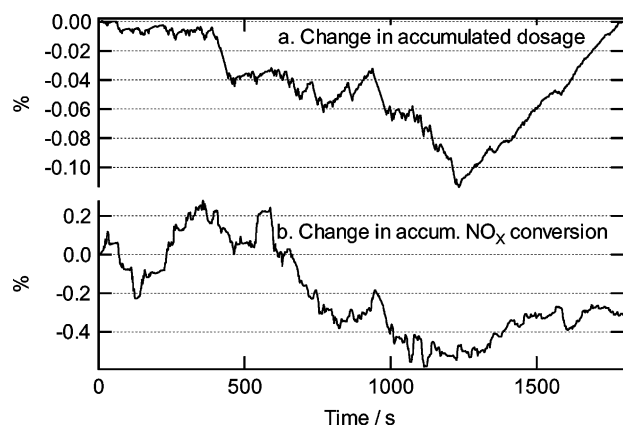


Fig. 7. Change in accumulated (a) dosage and (b) NO<sub>x</sub> conversion from the centre point of experimental design 1 to the centre point of experimental design 2.

reduced factorial design centred around these values was performed. In Fig. 7, the change in accumulated dosage and NO<sub>x</sub> conversion from the centre point of the first experimental design to the centre point of the second experimental design are shown. Part of the dosage is redistributed from the first 1240 s to the last 560 s of the ETC. This resulted in a 0.5% decrease in NO<sub>x</sub> conversion during the first 1240 s and a 0.2% increase during the last 560 s.

In the second experimental design, the influences of  $P_0$ ,  $n_S$  and  $k_1$  were studied. In Table 2, the values of the studied parameters and the obtained responses are listed.

Least squares fitting resulted in the following linear model:

$$\hat{y}_2 = 33.50 + 0.1263x_{21} + 0.1338x_{22} - 0.3112x_{23} \quad (7)$$

Table 2  
Variables and responses for the second experimental design<sup>a</sup>

Variables			Normalised and centred variables			NO <sub>x</sub> conversion, y <sub>2</sub>
$P_0$	<i>n</i> <sub>S</sub>	<i>k</i> <sub>1</sub>	<i>x</i> <sub>21</sub>	<i>x</i> <sub>22</sub>	<i>x</i> <sub>23</sub> = <i>x</i> <sub>21</sub> <i>x</i> <sub>22</sub>	
0.0025	5	2	0	0	0	33.40
0	3	3	−1	−1	1	32.96
0	7	1	−1	1	−1	33.84
0.0050	3	1	1	−1	−1	33.83
0.0050	7	3	1	1	1	33.48

<sup>a</sup> Fixed parameters were  $T_B = 360^\circ\text{C}$  and  $k_2 = 0$ .  $x_{21}$ ,  $x_{22}$  and  $x_{23}$  represents the normalised and centred variables  $P_0$ ,  $n_S$  and  $k_1$ , respectively.

Table 3  
Variables and responses for the experiments in the direction of the steepest ascent after the second experimental design<sup>a</sup>

Steps	Variables			NO <sub>x</sub> conversion
	$P_0$	<i>n</i> <sub>S</sub>	<i>k</i> <sub>1</sub>	
Δ	0.0010	1.86	−1	–
Centre point	0.0025	5.00	2	33.40
Centre + Δ	0.0035	5.86	1	34.76
Centre + 2Δ	0.0045	6.72	0	34.77
Centre + 3Δ	0.0055	7.58	−1	34.58

<sup>a</sup> Fixed parameters were  $T_B = 360^\circ\text{C}$  and  $k_2 = 0$ .

The second model (Eq. (7)) indicated that  $P_0$  and  $n_S$  had a positive influence and that  $k_1$  had a negative influence on the NO<sub>x</sub> conversion. Experiments were performed where the parameters were changed in the direction of the steepest ascent. The step size was chosen corresponding to a change by −1 for  $k_1$ . All parameters for the experiments and the corresponding NO<sub>x</sub> conversions are listed in Table 3.

In Fig. 8, the change in accumulated dosage and NO<sub>x</sub> conversion for the steps in the direction of the steepest ascent are shown. For each step the dosage becomes less dependent on the NO<sub>x</sub> flow. This results in marked decreases of the dosage especially around 400 and 950 s where there are high and sustained NO<sub>x</sub> flows and simultaneously high temperatures. The dosage increases at locations where the NO<sub>x</sub> flow is low and particularly when the temperature is high. This is most obvious between 1240 and 1560 s. The gain in NO<sub>x</sub> conversion is obtained during the first 180 s, between 330 and 390 s, 740 and 1040 s and from 1240 s to the end of the cycle. There is very little difference between the three experiments during the first 740 s. For the first step the gain

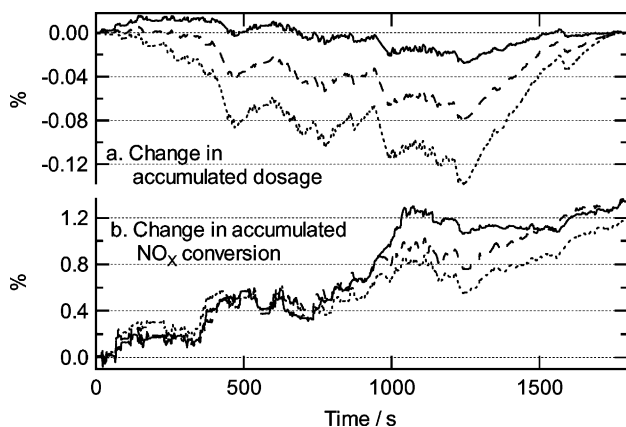


Fig. 8. Change in accumulated (a) dosage and (b)  $\text{NO}_x$  conversion for step 1 (solid), 2 (dashed) and 3 (dotted) in the direction of the steepest ascent after the second experimental design.

between 740 and 1040 s is larger than for the second step and the gain for the second step is somewhat larger than for the third step. For the second and third step there is a gain in  $\text{NO}_x$  conversion from 1240 s to the end of the cycle. For the first step the  $\text{NO}_x$  conversion remains almost unchanged between 1240 and 1560 s and a gain is observed from 1560 s to the end of the cycle. The total  $\text{NO}_x$  conversion was highest for the second step, but the difference in  $\text{NO}_x$  conversion between the first and the second step was only 0.01%.

It was decided that the next experimental design should be centred around the parameters in the second step, i.e.  $P_0 = 0.0045$ ,  $n_S = 6.72$  and  $k_1 = 0$ . However, by mistake the new experimental design was instead centred around  $P_0 = 0.0055$ ,  $n_S = 7.58$  and  $k_1 = 0$ . In Fig. 9, the change in accumulated dosage and  $\text{NO}_x$  conversion from the centre point of the second experimental design to the centre point of the third experimental design are shown. Compared to the steps in the direction of the steepest ascent after the second experimental design, the centre point of the third experimental design has a decreased dosage during the first 390 s of the cycle. This results in a 0.5% loss of  $\text{NO}_x$  conversion. From 1240 s to the end of the cycle the dosage is larger resulting in a somewhat larger gain in  $\text{NO}_x$  conversion.

In the third experimental design, the influences of  $P_0$ ,  $n_S$  and  $T_B$  were studied. In Table 4, the values of the studied parameters and the obtained responses are listed.

Table 4  
Variables and responses for the third experimental design<sup>a</sup>

Variables			Normalised and centred variables			$\text{NO}_x$ conversion, $y_3$
$P_0$	$n_S$	$T_B$ (°C)	$x_{31}$	$x_{32}$	$x_{33} = x_{31}x_{32}$	
0.0055	7.58	360	0	0	0	34.33
0.0030	5.08	380	-1	-1	1	34.29
0.0030	10.08	340	-1	1	-1	34.62
0.0080	5.08	340	1	-1	-1	34.82
0.0080	10.08	380	1	1	1	34.62

<sup>a</sup> Fixed parameters were  $k_1 = 0$  and  $k_2 = 0$ .  $x_{31}$ ,  $x_{32}$  and  $x_{33}$  represent the normalised and centred variables  $P_0$ ,  $n_S$  and  $T_B$ , respectively.

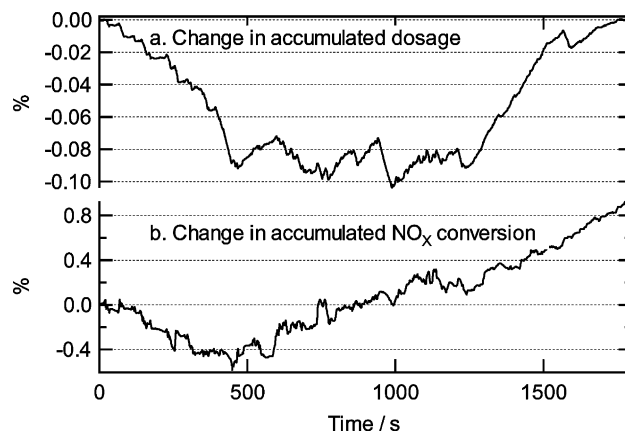


Fig. 9. Change in accumulated (a) dosage and (b)  $\text{NO}_x$  conversion from the centre point of experimental design 2 to the centre point of experimental design 3.

Table 5  
Variables and responses for the experiments in the direction of the steepest ascent after the third experimental design<sup>a</sup>

Steps	Variables			$\text{NO}_x$ conversion
	$P_0$	$n_S$	$T_B$ (°C)	
$\Delta$	0.0012	0.28	-10	-
Centre point	0.0055	7.58	360	34.33
Centre + $\Delta$	0.0067	7.86	350	35.17
Centre + 2 $\Delta$	0.0080	8.14	340	35.89
Centre + 3 $\Delta$	0.0092	8.41	330	36.06

<sup>a</sup> Fixed parameters were  $k_1 = 0$  and  $k_2 = 0$ .

Least squares fitting resulted in the following linear model:

$$\hat{y}_3 = 34.54 + 0.1325x_{31} + 0.0300x_{32} - 0.1350x_{33} \quad (8)$$

This model indicated that  $P_0$  had a strong positive influence, that  $n_S$  had a weak positive influence, and that  $T_B$  had a strong negative influence on the  $\text{NO}_x$  conversion. Experiments were again performed where the parameters were changed in the direction of the steepest ascent. The step size was chosen corresponding to a change by  $-10^\circ\text{C}$  for  $T_B$ . All parameters for the experiments and the corresponding  $\text{NO}_x$  conversions are listed in Table 5.

In Fig. 10, the change in accumulated dosage and  $\text{NO}_x$  conversion for the steps in the direction of the steepest



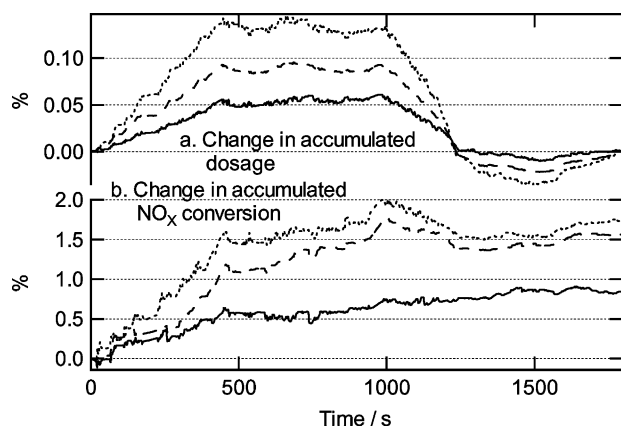


Fig. 10. Change in accumulated (a) dosage and (b)  $\text{NO}_x$  conversion for step 1 (solid), 2 (dashed) and 3 (dotted) in the direction of the steepest ascent after the third experimental design.

ascent are shown. For each step the base level fuel penalty,  $P_0$ , is increased, increasing the part of the dosage that is independent of the temperature. Simultaneously,  $T_B$  is decreased and  $n_S$  is increased, moving the temperature-dependent part of the dosage towards lower temperature and making the barrier steeper. The dosage is increased from the beginning of the cycle to 440 s and decreased between 970 and 1240 s. The largest gain in  $\text{NO}_x$  conversion is obtained during the first 440 s and the third step has the largest gain. For the first step there is a small gain in  $\text{NO}_x$  conversion during the complete cycle, but for the second and the third step there is a small loss between 970 and 1240 s. The total  $\text{NO}_x$  conversion was highest for the third step, but the difference in  $\text{NO}_x$  conversion between the second and the third step was only 0.17%. Further optimisation was performed, but no improved  $\text{NO}_x$  conversion was obtained.

In Fig. 11, the total change in accumulated dosage and  $\text{NO}_x$  conversion from the centre point of the first experimental design to the third step in the direction of the steepest ascent after the third experimental design are

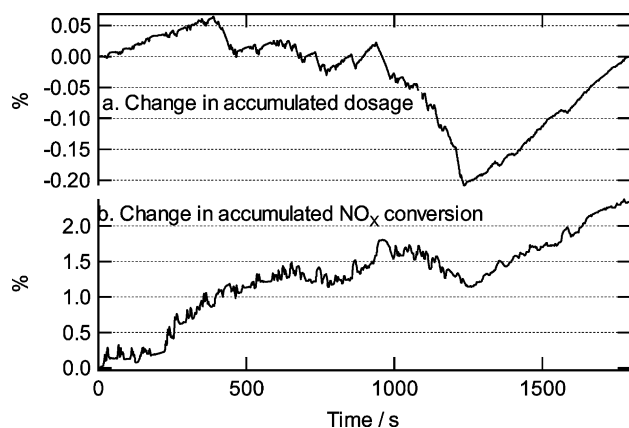


Fig. 11. Total change in accumulated (a) dosage and (b)  $\text{NO}_x$  conversion from the centre point of the first experimental design to the third step in the direction of the steepest ascent after the third experimental design.

shown. The optimisation has resulted in an increase of the dosage during the first 390 s of the cycle, where the temperature is relatively low, with a corresponding gain in  $\text{NO}_x$  conversion of 1%. The dosage has been decreased between 390–440 s and 940–990 s, where the  $\text{NO}_x$  flow is high and sustained and the temperature is high, with no loss in  $\text{NO}_x$  conversion. Between 990 and 1240 s the optimisation has resulted in a large decrease in the dosage with a corresponding loss of 0.6% in  $\text{NO}_x$  conversion. From 1240 s to the end of the cycle the dosage has been largely increased, with a corresponding gain of 1.2% in the  $\text{NO}_x$  conversion.

The optimisation shows that it is beneficial to distribute parts of the dosage at low and intermediate temperatures. This is an expected effect of the increased  $\text{NO}_2/\text{NO}$  ratio [16]. The largest gains in  $\text{NO}_x$  conversion are obtained in the beginning of the cycle, at low temperatures, and at the end of the cycle, at intermediate temperatures. At low temperatures a small, but appreciable, dosage is required to achieve an increased  $\text{NO}_x$  conversion. This requirement is met by using a sufficiently high value of  $P_0$ . At intermediate temperatures, a larger dosage is required to achieve an increased  $\text{NO}_x$  conversion. This requirement is met by using a sufficiently low value of  $T_B$ . The relatively high value of the steepness parameter,  $n_S$ , obtained in the optimisation, indicates that the transfer from the low temperature  $\text{NO}_x$  conversion to the intermediate temperature  $\text{NO}_x$  conversion occurs in a narrow temperature interval.

The optimisation resulted in a value of zero for  $k_1$ . This indicates that there is no gain in  $\text{NO}_x$  reduction by increasing hydrocarbon dosage at high  $\text{NO}_x$  flows. In fact, the optimisation showed that the dosage could be reduced during the high and sustained  $\text{NO}_x$  flows around 400 and 950 s without loss in  $\text{NO}_x$  conversion. The most probable explanation for this is the temperature delaying effect of the oxidation catalyst, as discussed above. Two separate tests were performed to investigate the effect of  $k_1$  and also the effect of  $k_2$ , thus using a linear and a quadratic dependence on the  $\text{NO}_x$  flow, respectively. In the first experiment  $k_1$  was changed from 0 to 1, starting from the optimised dosing strategy. In the second experiment  $k_2$  was changed from 0 to 218, corresponding to an equal change in  $k_0$  for both experiments. In Fig. 12, the changes in accumulated dosage and  $\text{NO}_x$  conversion are shown. In both experiments, the dosage is somewhat decreased during the first 390 s, mainly increased from 390 to 1240 s, and decreased from 1240 s to the end of the cycle. The difference in dosage between the experiments is that the changes are larger when the quadratic dependence is used. No major change in  $\text{NO}_x$  conversion occurs for either experiment during the first 1240 s. From 1240 s to the end of the cycle there is, however, a loss in  $\text{NO}_x$  conversion, with a larger loss for the quadratic dependence. It is thus clear that a linear or a higher order dependence of the  $\text{NO}_x$  flow is not beneficial when using an oxidation catalyst upstream the remainder of the system. However, a lower order dependence of the  $\text{NO}_x$  flow, as, e.g., a saturation function of the type  $k_a F_{\text{NO}_x} / (1 + k_b F_{\text{NO}_x})$ , may still be an interesting alternative.

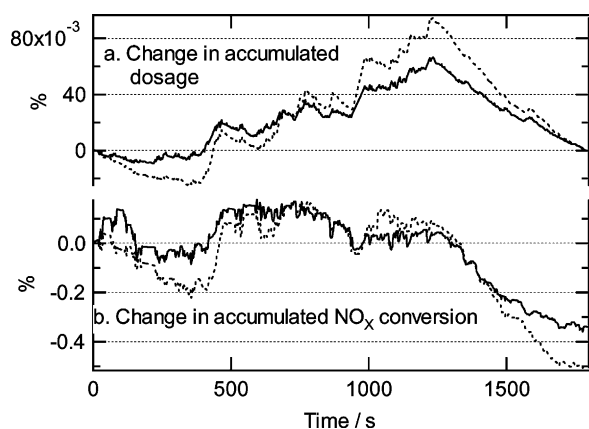


Fig. 12. Change in accumulated (a) dosage and (b)  $\text{NO}_x$  conversion when changing  $k_1$  from 0 to 1 (solid) and when changing  $k_2$  from 0 to 218 (dotted) in the optimised dosing strategy.

### 3.5. Introduction of multiple injectors

Multiple injectors, here to be understood as two injectors separated by one monolith, were thought to possess two potential advantages over a single injector set-up, namely with respect to firstly temperature effects and secondly HC distribution effects.

Regarding temperature effects, a transient system in a similar application shows large variations in temperatures along the system axis, as mentioned above and indicated in Fig. 3. It is thus likely that, during real use, not all parts of the catalyst will have temperatures corresponding to the activity window. Multiple injectors would, therefore, add the possibility of injecting HC upstream monoliths having an appropriate temperature, leaving monoliths of lower temperatures without reducing agent.

Concerning HC distribution effects, an even and appropriate coverage of the reducing agent is essential for an optimal catalytic reduction. Too high HC concentrations lead to lower relative HC conversion due to lack of catalyst surface oxygen, and thereby also lead to lower relative  $\text{NO}_x$  conversion [15]. An appropriate coverage can be obtained via multiple reductant injection, yielding relatively low HC concentrations locally despite large HC dosage globally.

Against the mentioned advantages with multiple injector set-ups stand two major disadvantages. Firstly, a second injector adds components and complexity to the exhaust gas system, and thus the cost increases. Secondly, HC introduced via an injector situated downstream any catalyst will have less residence time to interact with the remaining catalyst and may also be flushed out without reacting in case of high exhaust gas flows. The result can be larger HC, CO, and, depending on system appearance,  $\text{N}_2\text{O}$  emissions [15].

In Fig. 13a, the advantages and disadvantages of multiple injector set-ups can be recognised, knowing the characteristics of the test cycle. The reference strategy, with a distribution factor of 0 (single injector operation), here forms the baseline to which other results are compared. In-

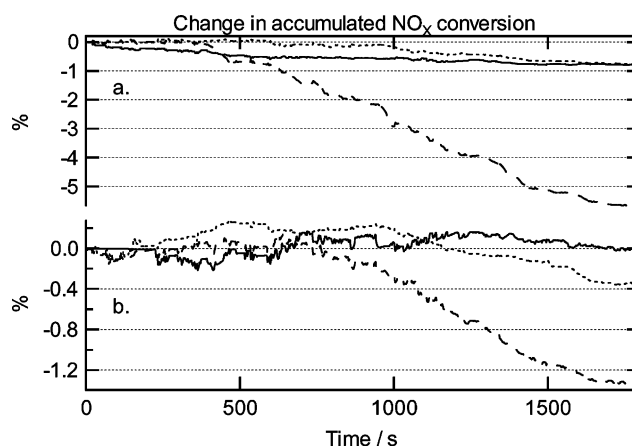


Fig. 13. Change accumulated in  $\text{NO}_x$  conversion: (a) when changing  $f_D$  from 0 to 0.1 (solid), to 0.2 (dotted) and to 1.0 (dashed) using the reference dosing strategy and (b) when changing  $f_D$  from 0 to 0.1 (solid), to 0.2 (dotted) and to 0.4 (dashed) using the optimised dosing strategy.

roducing a second injector and a distribution factor of 0.1 is not evidently of any larger benefit, regardless of the conditions in the cycle. The overall result for the whole cycle is, within the experimental error, identical to the one-injector set-up result. Doubling the distribution factor to 0.2 shows an interesting effect. The  $\text{NO}_x$  conversion during the first 600 s of the cycle, mainly consisting of low mass flow operation of the engine, is slightly positive. The last 1200 s of the cycle, however, show a clear negative trend, causing the overall result to be negative. Increasing the distribution factor further is of no essential gain at any part of the cycle, but strongly negative during the last 1000 s of the cycle. Concerning the optimised strategy, the corresponding graph is found in Fig. 13b. Firstly, one can note that a distribution factor of 0.1 gives a neutral result in total, and even during the cycle deviates little from the single injector reference. A distribution factor of 0.2 gives a visibly positive effect of the first 500 s, a neutral effect 500–1000 s and a negative effect 1000–1800 s. Increasing the distribution factor further is of no essential gain at any part of the cycle, but strongly negative during the last 1000 s of the cycle. These effects show that a distribution of the reducing agent along the monolith axis indeed is positive under certain circumstances, and, consistent with the above reasoning, mainly at low space velocities. Thus, there is an indication of the usefulness in some applications, if, however, not under such as represented by the ETC.

## 4. Summary and conclusions

The introduction of an oxidation catalyst upstream of the injector results in a temperature levelling and delay that reduces the potential for  $\text{NO}_x$  reduction during occasions with simultaneous high temperatures and high  $\text{NO}_x$  flows. The increased  $\text{NO}_2/\text{NO}$  ratio obtained with the oxidation

catalyst is beneficial at low and intermediate temperatures if the reductant dosage is large enough. In accordance, the optimisation of the dosing strategy shows that a considerable part of the reducing agent should be distributed at low and intermediate temperatures. The most important variable in the dosing strategy is the catalyst temperature. Weighting reductant dosage towards high  $\text{NO}_x$  flows showed no beneficial effect. An alternative to the linear and quadratic dependence could be to use a saturation function. The dynamics of the system indicates that the reducing agent should be distributed smoothly rather than instantly be adjusted to the driving conditions. This in turn indicates that a dosage exclusively proportional to the momentary fuel consumption is unfavourable. Using two injectors may have small beneficial effects at low mass flows. However, at high mass flows the shortened residence time for the reducing agent from the second injector has a strongly negative influence on  $\text{NO}_x$  reduction performance.

### Acknowledgements

Thanks to Prof. Gunnar Lundholm for providing the engine rig, Johnson Matthey for providing catalysts, Scania CV AB and Volvo Truck Corp., for their contributions to the project, Bengt Cyrén for assistance with the implementation of models and control of the pilot rig, Jan-Erik Everitt and Tom Hademark for practical assistance during tests. STEM, the Swedish National Energy Administration, is gratefully acknowledged for the financial support.

### References

- [1] M.D. Arimidis, T. Zhang, R.J. Farrauto, *Appl. Catal. B Environ.* 10 (1996) 203.
- [2] V.I. Părvulescu, P. Grange, B. Delmon, *Catal. Today* 46 (1998) 233.
- [3] K. Ogasawara, G. Muramatsu, S. Makino, *JSAE Rev.* 16 (1995) 61.
- [4] G.W. Rice, M. Deeba, J.S. Feeley, *SAE Technical Papers* 962043, Soc. Automot. Eng.
- [5] K. Katoh, Y. Kosaki, T. Watanabe, M. Funabiki, *SAE Technical Papers* 980931, Soc. Automot. Eng.
- [6] P. Ciambelli, P. Corbo, M. Gambino, F. Migliardini, *Stud. Surf. Sci. Catal.* 116 (1998) 307.
- [7] A. Peters, H.-J. Langer, B. Joki, W. Müller, H. Klein, K. Ostgathe, *SAE Technical Papers* 980191, Soc. Automot. Eng.
- [8] M.J. Heimrich, *SAE Technical Papers* 970755, Soc. Automot. Eng.
- [9] M. Kawanami, A. Okomura, M. Horiuchi, A. Schäfer-Sindlinger, K. Zerafa, *SAE Technical Papers* 961129, Soc. Automot. Eng.
- [10] C. Künkel, C.U.I. Odenbrand, B. Westerberg, B. Andersson, in: *Proceedings of the Internal Combustion Engines (ICE'97): Experiments and Modeling Conference*, Vol. 585, 1997, CNR, Istituto Motori, Naples.
- [11] M. Litorell, R. Allansson, A. Andreasson, S. Fredholm, P. Hawker, B. Johansson, P. Löf, G. Smedler, *SAE Technical Papers* 952489, Soc. Automot. Eng.
- [12] M. Iwamoto, T. Zengyo, A.M. Hernandez, H. Araki, *Appl. Catal. B Environ.* 17 (1998) 259.
- [13] K.A. Bethke, C. Li, M.C. Kung, B. Yang, H.H. Kung, *Catal. Lett.* 31 (1995) 287.
- [14] J.O. Petunchi, W.K. Hall, *Appl. Catal. B Environ.* 2 (1993) L17.
- [15] C. Künkel, C.U.I. Odenbrand, B. Westerberg, *SAE Technical Papers* 1999-01-3563, Soc. Automot. Eng.
- [16] B. Westerberg, B. Andersson, C. Künkel, C.U.I. Odenbrand, *Stud. Surf. Sci. Catal.* 116 (1998) 317.
- [17] B. Westerberg, C. Künkel, C.U.I. Odenbrand, *Chem. Eng. J.*, submitted for publication.